



Optimization of open cold-formed steel sections based on shape grammar

J.M.S Franco¹, E.M. Batista², A. Landesmann³

Abstract

The main goal of the present research is to find innovative and appropriate CFS shapes, improving its structural behavior at the same time that are manufacturable and, if possible, cost saving. Open cold-formed steel sections (CFS) optimization is obtained by integration of four investigation fields: (i) modeling the search domain, (ii) designing the fitness functions, (iii) applying Artificial Intelligence and (iv) computational implementation and visualization integrates the three other investigation fields. The paper focuses innovative application of Shape Grammar formalism, addressed to easy modeling of feasible CFS sections. The original developed algorithm is identified as CFS-Language - composed by a set of sentences translating each step of manufacturing by cold-forming - which was combined with Genetic Algorithm in order to select adequate shape, in accordance with previously selected objectives (Pareto's Front). The results of the analysis for three fitness functions are presented: (i) axial compression and (ii) flexural strength with the help of the Direct Strength Method and (iii) manufacturing costs. CFS-language was firstly developed in a CAD platform, further translated to MATLAB code and finally integrated with GA procedure inside the open-source code CUFSM (v.4.0.5) for buckling analysis based on constrained finite strip method. Based on the above described methodology, CFS shapes were generated by combining fitness functions and geometric modeling algorithms through Genetic Algorithm. The paper presents in detail the developed CFS-language, shows how the computational algorithms were integrated and finally presents the results of illustrative examples.

1. Introduction

Design product for cold-formed steel profiles (CFS) is a multidisciplinary optimization with structural, manufacturing and assembling requirements. The challenge is to decide how to fold a flat plate of constant dimensions in order to get major values of strength and to reduce manufacturing costs. This investigation has four branches: (i) search domain modeling defines the set of all valid shapes for a specific application and just these, (ii) design of objective

¹ Postdoctoral Researcher, Civil Engineering Program, COPPE, Federal University of Rio de Janeiro, <juarezfranco@coc.ufrj.br>

² Associate Professor, Civil Engineering Program, COPPE, Federal University of Rio de Janeiro, <batista@coc.ufrj.br>

³ Associate Professor, Civil Engineering Program, COPPE, Federal University of Rio de Janeiro, <alandes@coc.ufrj.br>

function evaluates shape fitness, (iii) some Artificial Intelligence (AI) technique is required to improve fitness and (iv) computational implementation and visualization integrates the three other investigation fields. This paper presents a search domain modeling for CFS design product based on Shape Grammar (SG), where manufacturing procedures are identified in order to get geometrical rules for shape drawing. SG is a parametric modeling technique developed at MIT (Gips 1972) and is addressed to different kinds of design product (Gips 1999). SG is often related as Artificial Intelligence approach, but is not an optimization algorithm. CFS-language is an original SG implementation associated with a Genetic Algorithm (GA) and addressed to CFS strength improvement. CFS search domain subsets assume variables sizes from a few elements until very large sets. Crashing of GA on this last kind of domains is expected and this behavior was observed in this work. Despite of this, where engineering experience has guided the choice of subsets of search domain, tests have presented meaningful improvement of fitness.

2. CFS search domain modeling by Shape Grammar

Parameterizing a product is to attribute a vector of real numbers to the description of a particular case inside a family of shapes. For example, just one parameter $x = \{x \in \mathbb{R}: 0 < x < 1\}$ is enough to describe any shape among all possible angle sections in Figure 1, where perimeter p and thickness t are constants and cold bending radius is ignored. Angle section is an example of one of three kinds of CFS search domain illustrated in Fig. 2: (i) set C are fixed typologies, (ii) set B are constrained free-form and (iii) set A are free-form, where $C \subset B \subset A$.

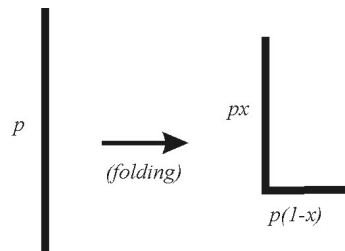


Figure 1: "Angle section" parameterization

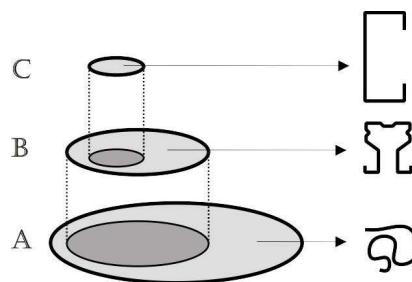


Figure 2: Fundamental CFS search's subdomains.

2.1 Precedent works

Optimization of cold-formed steel profiles from fixed typologies (set C in Fig. 2) has been investigated by almost two decades. Karim (1999) as performed hat-shape beams section optimization by Neural Networks and effective width concept to compute the capacities of shapes; Tran (2006) has optimized channel sections by the trust-region method based on the failure modes of yielding strength, deflection

limitation, local buckling, distortional buckling and lateral-torsional buckling by a standard MATLAB® optimization tool.

Free-form is a more recent investigation on CFS optimization (set *A* in Fig. 2). Leng (2011) proposed a search domain based on discrete shapes by constant number of elements with equal length, where angles between adjacent segments are variables and this vector of angles is a chromosome for GA and other AI algorithms. Resulting shapes (as exemplified in Fig. 3a) present a meaningful improvement of strength, but require a great effort for manufacturing and assembling. On other hand, important characteristics of CFS manufacturing are not included, as cold bending radius and intermediate stiffeners. Gilbert (2012a, 2012b) developed a shape generator based on recombination of random open discrete shapes, a very interesting GA approach where operators are applied over phenotype. However, resulting shapes are also difficult to manufacture, as presented in Fig. 3b.

Leng (2013) proposed a generator with manufacturing constraints. His work represents a great advance on constrained free-form CFS optimization, where almost all CFS characteristics are included on shape generation (Fig. 3c), but the domain is still limited by constant number of bent corners. In the present research, the modeling of a constrained free form search domain for CFS (set *B* on Fig. 2) is based on SG and offers three main advantages: (i) the algorithm is quite simple, (ii) the search domain is complete for any selected machinery operations and (iii) easiness to choice subsets from complete domain addressed to specific applications.

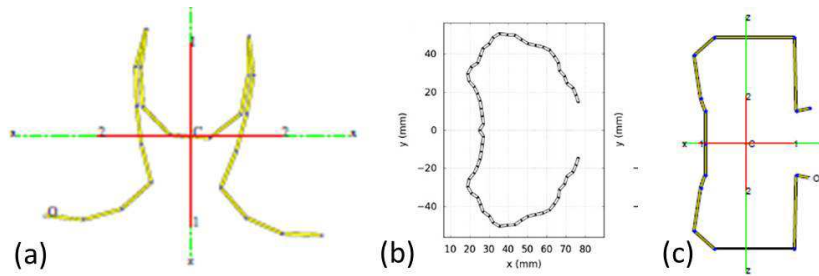


Figure 3: Precedents work on CFS search domain modeling: (a) (Leng *et.al.* 2011), (b) (Gilbert 2012a, Gilbert 2012b), (c) (Leng *et.al.* 2013).

2.2 Implementation

A manufacturable shape has its origin from a rectangular thin steel plate, subjected to a finite sequence of geometric transformations by cold-forming process. The generic sequence of these transformations is named vector φ ; angles between consecutive walls are named vector θ ; a third vector κ indicates proportion between walls and vector ρ represents radius of folded corner. Therefore, a generic shape w is represented by Eq. 1:

$$w = w(\varphi, \kappa, \theta, \rho) \quad (1)$$

The Shape Grammar approach defines all possible w like CFS language. The methodology closely follows the original model of generative grammars laid out in Chomsky (1972) to describe syntactic features of natural languages and the geometrical version of this grammar (Gips 1972), where “language” and “grammar” are mathematical concepts derived from the theory of groups. The CFS language is a set of sentences, each being finite in length and

constructed out with a finite set of symbols called the CFS Alphabet. Each symbol is a different instruction for shape generation, as presented in Table 1.

All cold-formed member manufacture starts from a flat steel sheet that is transformed into a new shape through folding operations. This process is represented by a **rewrite system**, where a set of rules changes substrings along a finite sequence of procedures. Alphabet and rules must be derived from a finite set of sentences called **corpus**. Cold-formed steel member structural design standards and codes deal with usual shapes illustrated in Fig. 4 and provide a corpus for the development of the CFS language.

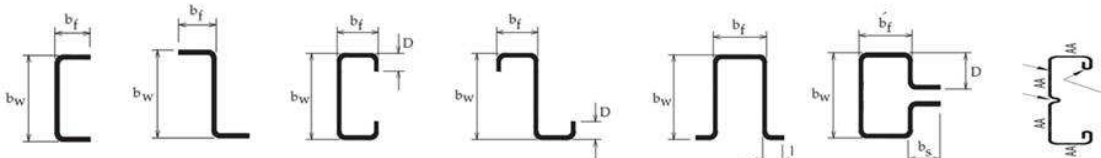


Figure 4: Usual shapes provisioned by cold-formed steel member structural design standards and codes.

The proposed CFS grammar is a device for producing all grammatical sequences of the CFS language and no ungrammatical ones. This approach inherits the Chomsky's (1972) model warnings: (i) there is no statistical approximation (whether a sentence is grammatically correct or not) and (ii) the grammatical notion cannot be identified with “meaningful”. First item means that it is impossible to generate a shape w by CFS grammar if it does not follow the manufacturing rules; second item is important because a valid sequence of symbols may result in cross-walled shapes. A semantic CFS algorithm has been included to identify and exclude these meaningless geometries. An unfolded plate is called axiom and valid transformations are productions or grammatical rules interpreted as *rewrite X as Y*, as presented in Table 2. Fig. 5 shows six rules obtained from C. Any shape w derived from the axiom following this set of rules is a derivation of sentence w .

Derivation by the rewrite system based on characters produces strings difficult to be read by human eyes. For example, a simple lipped channel derivation based on Tables 1 and 2 looks like the following, where two derivations are enough to generate a string representing it, but none particular shape is understood from these strings by “naked eyes”:

Axiom:	+F
derivation 1:	+{F(_f.fd.f.f.F)_f.fd.f.f.F}
derivation 2:	+{F(_f.fd.f.f.{F(_f.fd.f.f.F)_f.fd.f.f.F})_f.fd.f.f.F}

Many Computer Graphics (CG) applications offer scripting languages for simple grammar deployment by turtle concept (Prusinkiewicz 1990). The turtle is represented by a triplet $(x; y; \alpha)$, where the Cartesian coordinates $(x; y)$ represent the cursor's current position and its facing is oriented by angle α , called heading. Given an initial direction and step size, the turtle responds to commands represented by symbols included in Table 1.

Table 1: CFS alphabet end geometric interpretation.

CFS Alphabet	Geometric Interpretation
1. F	1. Wall
2. V	2. Stiffener
3. +	3. Angle between walls
4. *	4. Positive angle increment between stiffener walls
5. %	5. Negative angle increment between stiffener walls
6. [6. Start wall before a folding
7.]	7. End wall before a folding
8. <	8. Start wall after a folding
9. >	9. End wall after a folding
10. {	10. Start wall with two foldings
11. }	11. End wall with two foldings
12. (12. Start wall between two foldings
13.)	13. End wall between two foldings
14. F	14. Wall inside bending radius
15. .	15. Increment angle between walls inside curve
16. d	16. Computes arch length
17. u	17. Insert cold bending radius

Table 2: CFS grammar set of rules

CFS rules	Geometric Interpretation
1. $F \rightarrow F$	1. Keep this wall the same
2. $F \rightarrow [F] < uF >$	2. Fold wall at a single point
3. $F \rightarrow \{F(uF)uF\}$	3. Fold wall at two points
4. $F \rightarrow [F] < \% v^{**} v \% F >$	4. Apply a two-walled stiffener
5. $F \rightarrow \{F(\% v^{**} v v^{**} v \% F)\}$	5. Apply a three-walled stiffener
6. $u \rightarrow f:f d:f:f$	6. Apply cold bending folding

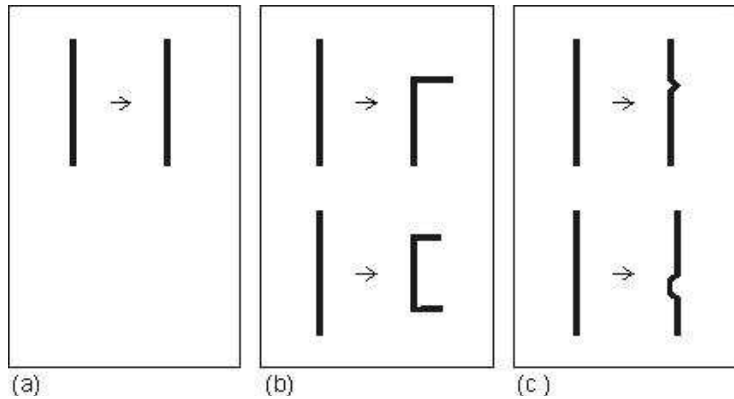


Figure 5: Set rules for CFS grammar: (a) identity, (b) folding and (c) intermediate stiffeners

3. Design of objective function

Design of CFS as a product implies simultaneous objectives, as maximum strength and minimal costs. In fact, an exact function $C_M(w)$ for manufacturing costs is dependent of variables like specific machinery, scale of production and other particular conditions of each manufacturer. For simplicity, as a first step, this work adopts $C_M(w)$ as a linear function of number of foldings, with the purpose to demonstrate the possibility to employ $C_M(w)$ in CFS multi-objective optimization as a general principle. On the other

hand, strength computation is based on many decades of international research and represented in this work by the functions in Eq. 2:

$$\begin{aligned} \text{Axial force: } w &\rightarrow H(w) \rightarrow N_{cR}(H(w)) \\ \text{Bending moment: } w &\rightarrow H(w) \rightarrow M_R(H(w)) \end{aligned} \quad (2)$$

where H is the buckling analysis procedure and provides critical loads associated with buckling deformation modes: Local (L), Global (G) and Distortional (D); N_{cR} provides nominal axial strength; M_R provides nominal flexural strength. Computational solvers for H are essential and free shared tools may be found. The notation of composite functions $N_{cR}(H(w))$ and $M_R(H(w))$ will be simplified to $N_{cR}(w)$ and $M_R(w)$.

3.1 Step 1: Elastic buckling analysis by FSM

Thin-walled structural members are sensitive to elastic buckling phenomena affecting its behavior, failure mechanism and final strength. This is the case of cold-formed steel members, which develop failure by combining elastic buckling deformation with material yielding and oblige the designer to recognize the dominant deformation with the help of previous elastic buckling analysis. Open cross-section thin-walled members may follow three main buckling modes, as illustrated in Fig. 6: (i) local buckling (L), in close correspondence with uniaxially compressed rectangular plates; (ii) distortional buckling (D), a combination of local plate bending with lateral displacements of almost one bent corner of the section and (iii) global buckling (G), which includes flexural, torsional or flexural-torsional buckling modes. The former (L) develops with short longitudinal half-wave lengths (of the order of the larger cross-section wall width b_w), distortional (D) with longitudinal half-waves longer than local mode and finally the global buckling modes (G) developing much longer half-waves, in many cases as long as the member's length (this is the case of member with pinned-pinned end condition). The lower buckling load identifies the critical one and its mode deformation will control the member's behavior with increasing amplification until yielding lines develop and promote localized failure. In addition, different buckling modes may develop in elastic interaction especially in the present case of thin-walled cold-formed members, obliging researchers to acquire in deep comprehension of the phenomenon in order to find accurate strength equation addressed to practical structural design.

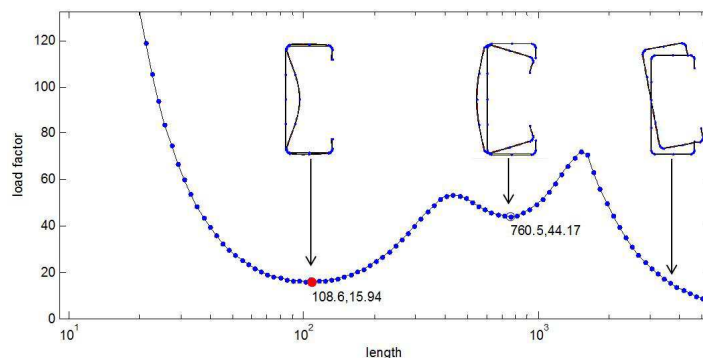


Figure 6: Results of the buckling analysis by finite strip method: Local (L), Distortional (D) and Global (G) buckling modes from CUFSM computational program.

Elastic buckling and strength of cold-formed steel members are investigated in close combination of the theory of elastic stability with numerical and experimental analysis. Nowadays, based on decades of

international research results in this field, the direct strength method (DSM) (Schafer 2006) is recognized as the one combining simplicity and accuracy allowing direct strength computation of buckling modes interaction based on equations which have been extensively calibrated with experimental results. Furthermore, as the nature of the failure of thin-walled members is associated with the above cited buckling modes, all DSM equations are based on the buckling loads respectively associated with axial compression N or bending moment M of the CFS member, i.e.: (i) local buckling N_L and M_L , (ii) distortional buckling N_{dist} and M_{dist} , (iii) global buckling N_e and M_e . Buckling modal identification requires buckling analysis solutions based on the large eigenvalues problem. In particular, the Finite Strip Method (FSM) and the Generalized Beam Theory (GBT) are the most efficient methods to solve CFS members for elastic buckling; the former is applied in the present investigation with the help of the free share computational program CUFSM (Schafer and Adány 2006). An open MATLAB® compiler source code, CUFSM allows buckling analysis of any type of CFS typology. Although GBT offers excellent results of buckling analysis, for example by means of the GBTUL (Bebiano *et.al.* 2008) computational program, FSM-based computational tool CUFSM offers an easy access to its open code allowing user to develop programming according to its own interest and necessities, which is the case of the present investigation. Critical load (or load factor) of each buckling mode (L and D) are given by the minimum points as shown in Fig. 6.

3.2 Step2: strength computation by DSM

Member's strength and its failure mode is a combination of elastic buckling and plasticity spread (yielding lines). Therefore, load factor derived from CUFSM (or GBTUL) solver for buckling analysis of thin-walled members are input to simple formulae provisioned by the direct strength method (AISI S100-2007). In this condition, the DSM-based optimization procedure explicitly requires a computational tool such as CUFSM for inputs, observed that the strength is accurately computed for single axial compression or bending loading, with no specific rule or equation for axial compression and bending moment combination as those of beam-column member. The DSM strength equations for axial compression are presented in the following and include global, local, distortional buckling as well as local-global buckling interaction. The nominal axial strength for flexural, torsional or torsional-flexural buckling related to global mode G is function of slenderness factor λ_0 in Eq. 3.

$$\lambda_0 = \sqrt{\frac{Af_y}{N_e}} \quad (3)$$

Where A is the cross-section area, f_y is the steel yield stress and N_e is the critical elastic buckling load - the minimum between flexural, torsional or torsional-flexural buckling loads. Once λ_0 is given, nominal axial strength related to global buckling is computed by Eq. 4.

$$\begin{aligned} N_{cRe} &= (0.658^{\lambda_0^2})Af_y \leftrightarrow \lambda_0 \leq 1.5 \\ N_{cRe} &= \left(\frac{0.877}{\lambda_0^2}\right)Af_y \leftrightarrow \lambda_0 > 1.5 \end{aligned} \quad (4)$$

The nominal axial strength for local buckling, also considering the effect of LG nonlinear interaction between local and global buckling depends on the slenderness factor λ_L in Eq. 5, where N_{cRe} is defined in Eq. 4 and N_L is the elastic local buckling load derived from CUFSM (or any other buckling solution).

$$\lambda_l = \sqrt{\frac{N_{cRe}}{N_l}} \quad (5)$$

Once λ_l is given, nominal axial strength for local buckling is computed by Eq. 6.

$$\begin{aligned} N_{cRI} &= N_{cRe} \leftrightarrow \lambda_l \leq 0.776 \\ N_{cRI} &= \left(1 - \frac{0.15}{\lambda_l^{0.8}}\right) \left(\frac{N_{cRe}}{\lambda_l^{0.8}}\right) \leftrightarrow \lambda_l > 0.776 \end{aligned} \quad (6)$$

The nominal axial strength for distortional buckling D is computed without any interaction with L or G buckling modes and depends of the slenderness factor λ_{dist} in Eq. 7, where N_{dist} is the critical elastic distortional buckling load derived from CUFSM (or any other buckling solution).

$$\lambda_{dist} = \sqrt{\frac{Af_y}{N_{dist}}} \quad (7)$$

Once λ_{dist} is given, nominal axial strength for distortional buckling is computed by Eq. 8.

$$\begin{aligned} N_{cRdist} &= Af_y \leftrightarrow \lambda_{dist} \leq 0.561 \\ N_{cRdist} &= \left(1 - \frac{0.25}{\lambda_{dist}^{1.2}}\right) \left(\frac{Af_y}{\lambda_{dist}^{1.2}}\right) \leftrightarrow \lambda_{dist} > 0.561 \end{aligned} \quad (8)$$

Finally, the nominal axial strength for a CFS member is defined as the minimum between the computed strength values by Eq. 9:

$$N_{cR} = \min(N_{cRe}, N_{cRI}, N_{cRdist}) \quad (9)$$

The nominal flexural strength for global buckling, namely the lateral-torsional buckling mode, depends on slenderness factor λ_0 in Eq. 10, where S is the elastic modulus of the section and M_e is the critical lateral-torsional buckling bending moment.

$$\lambda_0 = \sqrt{\frac{Sf_y}{M_e}} \quad (10)$$

Once λ_0 is given, nominal flexural strength for global buckling is computed by Eq. 11.

$$\begin{aligned}
M_{Re} &= Sf_y \leftrightarrow \lambda_0 \leq 0.6 \\
M_{Re} &= 1.11(1 - 0.278\lambda_0^2)Sf_y \leftrightarrow 0.6 < \lambda_0 < 1.336 \\
M_{Re} &= \frac{Sf_y}{\lambda_0^2} \leftrightarrow \lambda_0 \geq 1.336
\end{aligned} \tag{11}$$

The nominal flexural strength for local buckling including the effect of nonlinear interaction between local and global buckling, identified as *LG* interaction, depends on slenderness factor λ_L in Eq. 12, where M_{Re} is given by Eq. 11 and M_L is the elastic local buckling bending moment given by CUFSM (or any other buckling solution).

$$\lambda_L = \sqrt{\frac{M_{Re}}{M_L}} \tag{12}$$

Once λ_L is known, nominal flexural strength for local buckling is computed by Eq. 13.

$$\begin{aligned}
M_{Rl} &= M_{Re} \leftrightarrow \lambda_l \leq 0.776 \\
M_{Rl} &= \left(1 - \frac{0.15}{\lambda_l^{0.8}}\right) \left(\frac{M_{Re}}{\lambda_l^{0.8}}\right) \leftrightarrow \lambda_l > 0.776
\end{aligned} \tag{13}$$

The nominal flexural strength for distortional buckling in bending depends on slenderness factor λ_{dist} in Eq. 14, where M_{dist} is the critical elastic distortional buckling bending moment given by CUFSM (or any other buckling solution).

$$\lambda_{dist} = \sqrt{\frac{Sf_y}{M_{dist}}} \tag{14}$$

Once λ_{dist} is known, nominal flexural strength for distortional buckling is computed by Eq. 15.

$$\begin{aligned}
M_{Rdist} &= Sf_y \leftrightarrow \lambda_{dist} \leq 0.673 \\
M_{Rdist} &= \left(1 - \frac{0.22}{\lambda_{dist}}\right) \left(\frac{Sf_y}{\lambda_{dist}}\right) \leftrightarrow \lambda_{dist} > 0.673
\end{aligned} \tag{15}$$

Finally, the nominal flexural strength for a CFS member is defined as the minimum between the computed strength values in Eq. 16:

$$M_R = \min(M_{Re}, M_{Rl}, M_{Rdist}) \tag{16}$$

4. Genetic Algorithm NSGA-II

Since C_M , N_{cR} and M_R are defined, a multi-objective optimization is formalized by Eq. 17:

$$\begin{aligned} & \text{Maximize } N_{cR}(w) \\ & \text{Maximize } M_R(w) \\ & \text{Minimize } C_M(w) \\ & \text{Subject to } w \in B \end{aligned} \tag{17}$$

It remains a beam optimization when just $N_{cR}(w)$ is disabled; if $M_R(w)$ is disabled only, it becomes a column optimization; if equations of $N_{cR}(w)$ and $M_R(w)$ are enabled, it is a beam-column optimization, which requires an additional interaction equation enabling the evaluation of the beam-column strength. None of the feasible solutions allows simultaneous optimal results for all objectives on beam-column optimization problem, because it is expected that a better shape under axial compression will be different from another under flexural bending or a particular combination of compression and bending. There are many alternative algorithms to perform optimization. Genetic Algorithm (GA) is an adequate choice because it is able to operate over populations (sets) of solutions. In this work, the subset $P \subset B$ of best shapes found in Pareto's front by GA (Deb 2002) is defined as a shape library. Genetic algorithms have some well-known disadvantages like high computational costs and no guarantee of global maximum achievement.

Modified Non-Dominated Sorting Genetic Algorithm, NSGA-II (Seshadri *nd*) is a popular GA implementation where Pareto's front is a collection of non-dominated solutions. For this problem, a general shape $w(\varphi, \theta, \kappa, \rho)$ is codified by float numbers into chromosomes. Therefore, a chromosome is a p -dimensional vector, where p is the sum of φ , θ , κ and ρ vector dimensions and its evaluation results in n -dimensional vector f , where n is the number of objectives. For a minimization problem, w_1 is a non-dominated solution over w_2 if there is at least one entry on $f(w_1)$ that is smaller than the same position in $f(w_2)$. NSGA-II initializes the chromosomes using a random process. First, a population P of candidates $w(\varphi, \theta, \kappa, \rho)$ is started and all of them are evaluated. For each $p \in P$ two numbers are signed: (i) n_p , quantity of elements in P that dominates p and (ii) S_p , number of solutions dominated by p . All solutions where $n_p=0$ are located in the first front and are signed with rank = 1. Higher-order ranks are placed in successive fronts. Next step, solution's density into each front (crowding distance) is taken. Higher densities are related to smaller fitness in order to increase variability in population. NSGA-II uses ranking and crowding distance as fitness measures. Traditional GA crossover and mutation operators are applied until the stop criterion is reached (maximum number of generations specified by the user).

5. Results

The following numerical results have constant plate dimensions for all implemented examples: steel sheet thickness $t=1.0mm$, cold bending internal radius $r_i=3.0mm$, perimeter length (or plate width) $p=280.0mm$ and member length $L=1219.0mm$, for which a major number of cases with predominance of L and D buckling modes are expected. Nominal steel mechanical properties are Young Modulus $E=205.0GPa$, Poisson ratio $\nu=0.3$ and yield stress $f_y=300.0MPa$. Vector sizes of φ , θ , κ and ρ are dependents of maximum number of derivations specified. Folding numbers were limited from 2 to 17. Single rectangular plates and angle profiles, respectively null or one-fold, were excluded for stability considerations; higher number of folding operations represents a considerable increase in computational costs, thereby requesting higher performance computers and, in addition, it could generate impractical

solutions. The shape generator automatically divides 30.0mm wider wall elements by two for matrix analysis purposes (one intermediate node is included in the mid position of the element). Results have been classified in two blocks, (i) guided search, where some functional constraint is imposed to shape and (ii) free-form search, where manufacturing possibility is the only constraint.

5.1. Guided search

Let “sigma-and-neighborhood” be a shape optimization problem with functional constraint where at least one wall must be in vertical position (web element) with one middle intermediate stiffener. The proposed problem is called “sigma-and-neighborhood” because the traditional edge stiffened sigma shape shown in Fig. 7 is an adequate initial case for investigation. Other geometrical possibilities, including the consequences of changing angles between walls (Session 5.1.2) and the proportions among walls (Section 5.1.3), are also presented below. The CFS grammar demands manipulation of vectors θ and κ in order to solve the problems in Sessions 5.1.1 to 5.1.3, without requiring specific algorithms for the investigated shapes. In addition, the intermediate stiffener placed in the web was previously designed with constant geometry, thereby providing efficient stiffening in order to improve local buckling load.

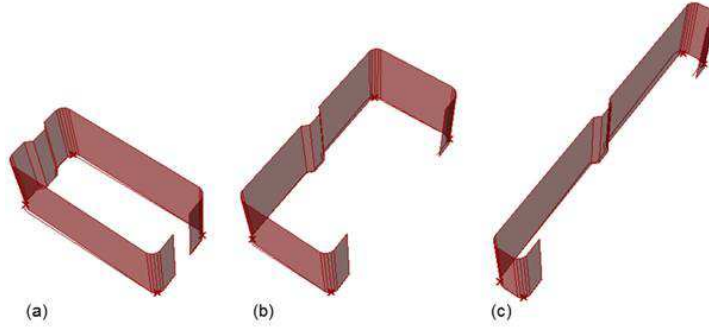


Figure 7: Geometrical models for Sigma shapes: (a) $\kappa_2=0.1$ (b) $\kappa_2=0.5$ and (c) $\kappa_2=0.9$

5.1.1 Sensitivity analysis on fixed typologies

Sigma shape “adds” an efficient intermediate stiffener at the middle point of the web of a lipped channel. Values for the parametric CFS grammar, are presented in Eq. 18. Position κ_2 (representing in this example the proportion between web and flange ($b_w/(b_w + 2b_f)$) for the sigma channel) is the variable to be evaluated, as shown in Fig. 8, where $\kappa_2=\{\kappa_2 \in R: 0.1 < \kappa_2 < 0.9\}$.

$$\begin{aligned}
 \varphi &= [3;1;3;1;1;1;5] \\
 \theta &= [-180;-90;-90;-90;-90;-90] \\
 \rho &= [3;3;3;3] \\
 \kappa &= [0.9; \kappa_2]
 \end{aligned} \tag{18}$$

Fifty values of κ_2 were assigned on a specified range and computed with a modified version of CUFSM. Checking N_{cR} and M_R in Fig. 8 reveals that columns maximum nominal axial strength at $\kappa_2=0.52$ and beams have maximum nominal flexural strength at $\kappa_2=0.7$. Selecting the “best solution” can be a difficult task for a beam-column design problem because N_{cR} and M_R have a conflict for $\kappa_2=\{\kappa_2 \in R: 0.52 < \kappa_2 < 0.7\}$: if N_{cR} is improved, M_R decreases.

This shape library (Fig. 8) is related to one variable for two objectives and could be a starting point for handwork beam-column design for which the bending moment effect is not predominant. As a

consequence, typical beam-column nonlinear behavior can be safely replaced by the linear interaction in Eq. 19 (ANBT 2009) (typically the case of trussed girders with joint eccentricities where bending moment develops with minor importance), where N_S and M_S are respectively the applied axial compression and bending moment.

$$\frac{N_S}{N_{cR}} + \frac{M_S}{M_R} \leq 1 \quad (19)$$

In this example, providing an intermediate web stiffener in Sigma shapes (as stated above, efficient intermediate stiffener was adopted improving the local buckling behavior and strength) induced a 54% increase in the maximum compressive axial strength N_{cR} , if compared with an equivalent lipped channel ($49/31.8=1.54$ at $\kappa_2=0.52$), and a 20% increase in the maximum bending moment strength ($3.35/2.8 = 1.20$ at $\kappa_2=0.7$)

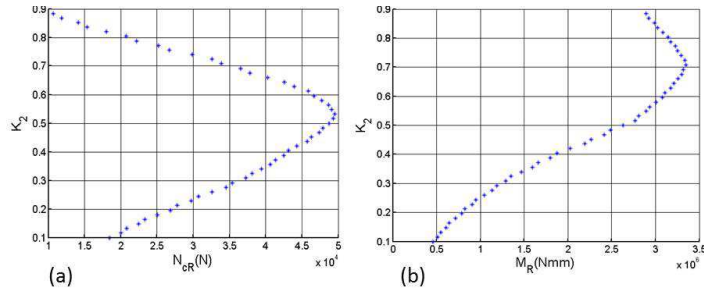


Figure 8: (a) Axial compression $N_{cR}(w)$ and (b) bending moment strength $M_R(w)$ as a function of parameter κ_2 for sigma shape.

5.1.2 Optimization with constant number of bent corners

Session 5.1.1 suggests that $\kappa_2=0.52$ for the highest strength shapes in the standard Sigma problem. This value has been assigned as constant to κ_2 in the present Session and vector θ was taken as variable. This problem is addressed to verify if the standard Sigma shape got in the past Session is an optimum solution. Five records of θ are manipulated to constraint one vertical wall and four angle variables on sigma shape. Eq. 20 indicate the vectors addressed in sigma typology, where $\theta_i = \{\theta_i \in R: -180 < \theta_i < 180\}$.

$$\begin{aligned} \varphi &= [3; 1; 3; 1; 1; 1; 5] \\ \theta &= [\theta_1, \theta_2, -(\theta_1 + \theta_2), \theta_4, \theta_5] \\ \rho &= [3; 3; 3; 3] \\ \kappa &= [0.9; 0.52] \end{aligned} \quad (20)$$

This domain includes 1.68×10^{10} possibilities. An exhaustive search requesting 1 second by analysis would take more than 540 years of continuous processing, instead of some hours by GA. Fig. 9 show that customized shapes have up to 9% axial strength improvement when compared with the best traditional Sigma shape with the same proportions among walls ($53.5/49=1.09$ from Figs. 8a and 9). The improvement means that standard Sigma shape is not an optimal solution if other solutions around “neighborhood” are considered. Fig. 9(b) shows four solutions taken from this shape library.

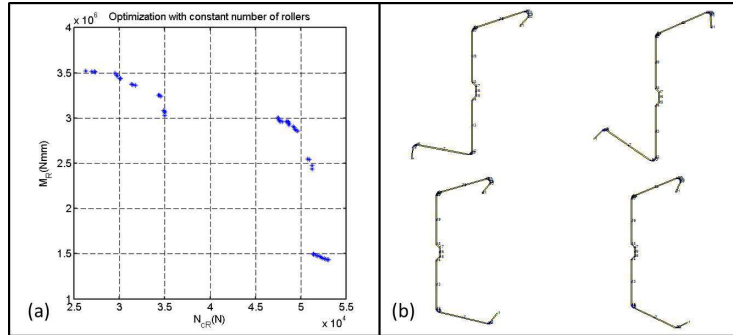


Figure 9: N_{CR} vs M_R Pareto's front for modified sigma shape.

5.1.3 Enlarged search domain on guided search

A wider domain than previous one in Session 5.1.2 was considered, including vectors κ and θ as variables. This domain has 1.68×10^{14} solutions and the unusual cost of "5.4 million years" to be solved based on exhaustive search with usual computer performance around 1 second per analysis. Fig. 10 shows that the maximum N_{CR} improves 16%, when compared with the best shape from Session 5.1.1 ($57/49=1.16$), and 6% when compared with the best shape from Session 5.1.2 ($57/53.5=1.06$). On the other hand, there is no improvement for M_R . Four shapes from this library are presented in Fig. 10(b).

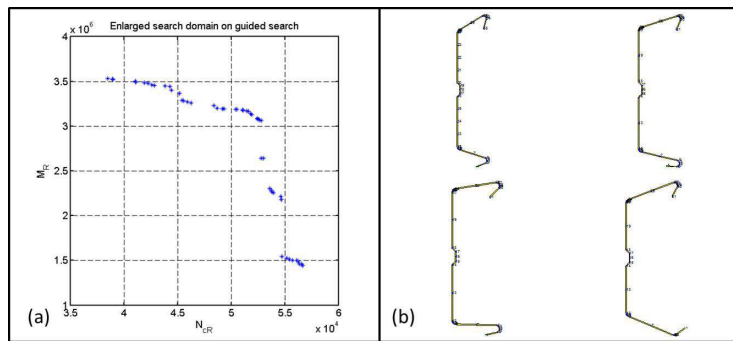


Figure 10: N_{CR} vs M_R Pareto's front for modified sigma shape.

Sessions 5.1.1 to 5.1.3 presented a progression from predefined shapes to previously undefined solutions developed with the help of Artificial Intelligence. These cases demonstrate how the experienced designer plays a fundamental role in CFS usual problems, allowing a very valuable initial input in optimization problems and, as a consequence, a reduction of the search domain to as close as possible to the optimal solution and consequently saving computational costs of the search.

5.2. Free-form constrained by manufacturing rules

Sessions 5.2.1 to 5.2.3 address problems without functional constraints or parameters defined by experience. These examples have no constructive purposes, but are valuable to (i) demonstrate the descriptive power of the CFS Grammar and (ii) verify GA's capacity to find previously known "optimal" solutions into a very large domain. Vectors ϕ , θ and κ were placed into chromosomes with 31 variables, resulting in a domain with 2.23×10^{55} elements. Optimized shapes of Sessions 5.1.1 to 5.1.3 are inside this domain and a GA would be able to find them or something better than useless or unnecessarily expensive shapes. All the following examples have exactly the same parameters in the Shape Grammar, according

to Eq. 21, and only differ in the specified goals fed into the Genetic Algorithm, where: $\varphi_i = \{\varphi_i \in \mathbb{R}: 1 \leq i \leq 5\}$; $\theta_i = \{\theta_i \in \mathbb{R}: -180 \leq \theta_i \leq 180\}$; $\kappa_i = \{\kappa_i \in \mathbb{R}: 0.1 \leq \kappa_i \leq 0.9\}$; $\rho_1 = 3$.

$$\begin{aligned}\varphi &= [\varphi_1, \dots, \varphi_7] \\ \theta &= [\theta_1, \dots, \theta_{17}] \\ \rho &= [\rho_1, \dots, \rho_{17}] \\ \kappa &= [\kappa_1, \dots, \kappa_7]\end{aligned}\tag{21}$$

5.2.1. Column optimization with cost function

Let $N \times C$ be an optimization problem where strength must be compared with manufacturing costs. GA has been configured to work with 100 individuals and an evolution process of 200 generations, the procedure has been repeated twice and the best shape library is presented in Fig. 11.

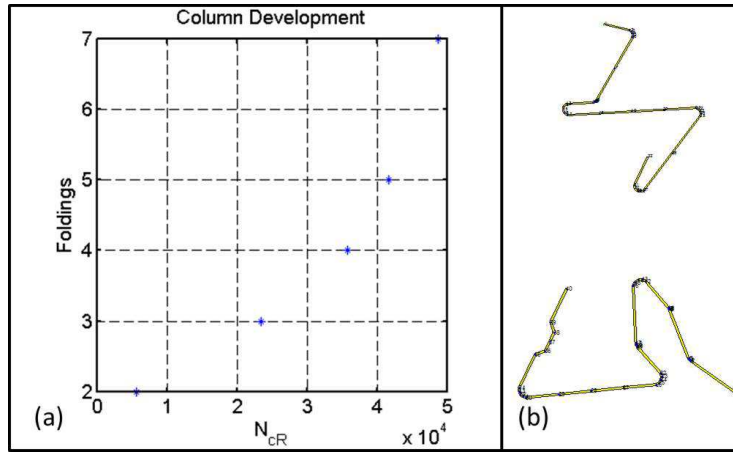


Figure 11: N_{CR} vs C_M Pareto's front for session 5.2.1

The highest strength into this shape library is 49.0kN. This value is equal to the standard Sigma channel in Session 5.1.1 ($49/49=1.00$). On the other hand, it is 14% lower than the best non-conventional shape in Session 5.1.3 ($49/57=0.86$). GA has failed to find an expected optimal solution without engineering experience to guide the choice of parameters and to reduce the domain size. Fig. 11(b) presents two of the solutions from this shape library. As expected in the design of members under axial compression, the proportion between major and minor inertia axis are close to unity ($I_1/I_2 \rightarrow 1$). Additionally, shear and centroidal centers became closer, with tendency to coincide, thus improving member efficiency for flexural-torsion.

5.2.2. Beam optimization with cost function

Let $M \times C$ be an optimization problem where strength must be compared with manufacturing costs. Solutions are supposed to be the best collection for flexural bending from 2 up to 6 foldings as presented in Fig. 12. The evolution pressure for minor costs decreased the trend for improved strengths and, consequently, the higher value of M_R (3.35kNm) is 4% lower than the corresponding result obtained in Session 5.1.3 ($3.35/3.5 = 0.96$). Note that Pareto contains just one solutions for each number of folding, suggesting the convergence of the GA towards a reduced set of shapes. Fig. 12(b) presents two solutions extracted from this shape library, which confirms the tendency of beam-like sections with a single web and large amount of material in the stiffened compressed flange side.

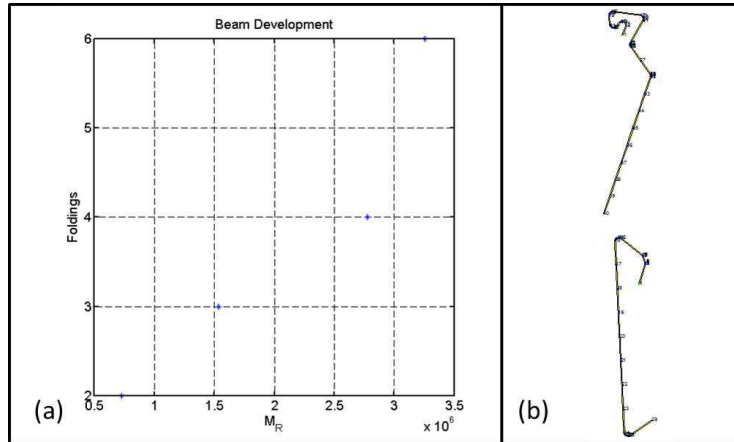


Figure 12: N_{cR} vs C_M Pareto's front for Session 5.2.2

5.2.3. Beam-column optimization with cost function

Let $M \times N \times C$ be an optimization problem without functional constraints for which the strength must be compared with manufacturing costs. Concerning combined bending and axial compression strength, linear interaction Eq. 19 is to be considered only if the non-linear beam-column amplification effect can be neglected. Visualization of the relationship between three goals requires the 3D graphic shown in Fig. 13, where N_{cR} vs M_R results were layered by the folding number. GA has been configured to work with 100 individuals and an evolution process of 200 generations; the procedure has been repeated twice and the best population elected. Higher strengths are compatible with the results obtained in Sessions 5.1.1 to 5.1.2. GA was not able to yield solutions with the same strength of Session 5.1.3, in which the domain was reduced by engineering experience. Furthermore, solutions without functional constraints are out of any practical scope and not able to be employed for practical purposes as can be confirmed in Fig. 13(b). The presented example shows at the same time GA's capabilities and limitations to organize solutions based on their fitness for different purposes. In addition, there are many other possibilities that can be explored using the proposed CFS grammar rules. These possibilities can be increased if one extends the grammar to include other rules, making it fit to address other engineering goals. Results thus suggest that other grammars for other goals can be developed, indicating that the application of shape grammars to the engineering domain has a great potential to be explored.

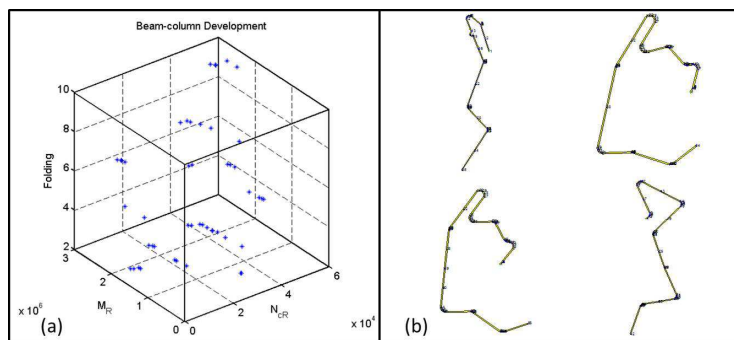


Figure 13: N_{cR} vs M_R vs C_M Pareto's front for Session 5.2.3.

FINAL REMARKS

Despite FSM limitations (Schafer and Ádány 2006) and low speed of MATLAB® compiler, CUFSM was proved to be an adequate choice for CFS optimization problems. Optimization of CFS shapes presents dichotomies that are produced by technical limitations. The first one opposes improving strength (i) for usual, feasible shapes with functional constraints and (ii) for unfeasible geometries without functional constraints. The main purpose of this paper is to present the development and the obtained results of a shape generator able to perform optimization for both cases with simple and flexible implementation. The proposed CFS Shape Grammar approach offers descriptive power, simplicity of implementation and easiness of customization. A second dichotomy is represented by Artificial Intelligence (AI) and professional engineering experience. CFS structural capability may show non-intuitive behavior and can surprise even experienced engineers, but there is no reason to believe that experience does not play an essential role in CFS optimization. Actually, experience strongly helps reducing search domain and computational costs of optimization, while adequate search algorithms and sensibility analysis may improve engineering decision. Technically, it is necessary to combine Shape Grammar, buckling analysis, strength computation and Genetic Algorithm (or other AI algorithm) into a more robust computational compiler. Finally, the improvement of the presented procedure also depends on the evolution of the strength computation capabilities as those proposed by the Direct Strength Method, which is under development, especially for the cases of buckling interaction LD, DG and LDG. None of them are considered inside design codes and standards prescriptions although many results are available from numerical and experimental investigation (Dinis 2011, Santos 2012, Dinis 2012). The same comment may be addressed regarding the case of steel thin-walled cold-formed beam-columns, which so far does not count with a confirmed DSM-based solution for the moment.

References

- ABNT NBR14762 (2009), “Design of steel structures with cold-formed members”, *Associação Brasileira de Normas Técnicas*, September 2009, Revision draft (in Portuguese).
- AISI S100-2007 (2007). “North American specification for the design of cold-formed steel members, Appendix 1: Design of cold-formed steel structural members using the Direct Strength Method”. *American Iron and Steel Institute*.
- Bebiano R., Pina P., Silvestre N., Camotim D., (2008) “GBTUL 1.0 β – Buckling and Vibration Analysis of Thin-Walled Members”, *DECivil/IST, Technical University of Lisbon*, (<http://www.civil.ist.utl.pt/gbt>).
- Chomsky, N., (1972) “Syntactic Structures”. 10 ed. The Hague, Mouton & Co.
- Deb, K., Pratap, A., Agarwal, S., and Meyarivan, T., (2002) “A fast elitist multiobjective genetic algorithm: NSGA-II”, *IEEE Transactions on Evolutionary Computation*, 6(2), 182-197.
- Dinis, P.B., Batista, E.M., Camotim, D., Santos E.S., (2012) “Local distortional global interaction in lipped channel columns: Experimental results, numerical simulations and design considerations” *Thin-Walled Structures* (61) 2-13.
- Dinis P.B., Batista E.M., Camotim D., Santos E.S., (2011) “Local/distortional/global mode coupling in fixed lipped channel columns: behavior and strength”, *Advanced steel construction* (7) 114-131.
- Gilbert, B.P., Savoyat, T.-M., Teh, L., (2012b) “Self-shape optimization application: optimization of cold-formed steel columns”, *Thin-Walled Structures* (60) 173-184.
- Gilbert, B.P., Teh, L., Guan. H., (2012a) “Self-shape optimization principles: Optimization of section capacity for thin-walled profiles”, *Thin-Walled Structures* (60) 194-204.
- Gips, J., (1999) “Computer implementation of shape grammars”. Invited paper, *Workshop on Shape Computation*, MIT.
- Gips, J., Stiny, G., (1972) “Shape Grammars and Generative Specification of Paiting and Sculpture”, Auerbach Publications, 125-135.
- Karim, A., Adeli, H., (1999) “Global optimum design of cold-formed steel hat-shape beams”. *Thin-Walled Structures* (35) 1218-1231.

- Leng, J., Guest, J.K., Schafer, B.W., (2011) "Shape optimization of cold-formed steel columns", *Thin-Walled Structures* (49) 1492-503.
- Leng, J., Guest, J.K., Schafer, B.W., Li, Z., (2013) "Shape optimization of cold-formed steel columns with manufacturing constraints and limited number of rollers", in *Proceedings of the Annual Stability Conference* (49) 313-331.
- Prusinkiewicz, P. and Lindenmayer, A., (1990) "The Algorithmic Beauty of Plants" New York: Springer-Verlag.
- Santos E.S., Batista, E.M., Camotim, D., (2012) "Experimental investigation concerning lipped channel columns undergoing local distortional global buckling mode interaction" *Thin-Walled Structures* (54) 19-34.
- Schafer B.W., (2006) "Designing cold-formed steel using the direct strength method" in *18th International Specialty Conference on Cold-Formed Steel Structures*
- Schafer B.W., Ádány, S., (2006) "Buckling analysis of cold-formed steel members using cufsm: conventional and constrained finite strip methods", in *18th International Specialty Conference on Cold-Formed Steel Structures*
- Seshadri, A., (nd) "Multi-objective optimization using evolutionary algorithms" (*report*).
- Tran, T., Li, L., (2006) "Global optimization of cold-formed steel channel sections". *Thin-Walled Structures* (44) 399-406.